ELSEVIER

Journal of Nuclear Materials 276 (2000) 178–185

journal of nuclear materials

www.elsevier.nl/locate/jnucmat

Comparison between radiation effects in some fcc and bcc metals irradiated with energetic heavy ions – a review

A. Iwase[a], S. Ishino[b,*]

[a] *Department of Materials Science, Japan Atomic Energy Research Institute, Tokai-mura, Naka-gun Ibaraki-ken 319-1195, Japan*
[b] *Department of Nuclear Engineering, Tokai University, 1117, Kitakaname, Hiratsuka-shi, Kanagawa-ken 259-1292, Japan*

Abstract

It has been reported that there are substantial differences in radiation effects in fcc copper and bcc iron. Whether these differences are due to the difference in crystal structure or not is the subject of the present paper. These differences have been discussed in terms of microstructure and mechanical property changes, whereas in the present paper, results of electrical resistivity measurements are discussed in terms of damage production cross sections, defect annihilation cross sections, damage efficiency and so on during and after various ion irradiations with wide energy ranges from 1 MeV to more than 100 MeV. For crucial discussion on the effect of the difference in crystal structure, nickel and iron are compared. These metals are allotted closely in the periodic table, with similar melting points and fairly strong electron–lattice coupling, both ferromagnetic and yet with different crystal structure. It may be concluded that as far as the damage production and defect annihilation cross sections and survival ratio are concerned, the difference in crystal structure is not an essential factor. Electronic energy deposition may play an important role even for low energy ions as well as for high energies. The effect of electronic energy deposition on defect clustering is discussed.

1. Introduction

There has been a considerable interest, in recent years, in radiation effects in metals and alloys particularly in differences and similarities of radiation effects among fcc, bcc and hcp metals [1]. Singh and Evans have compiled and evaluated a number of experimental results of radiation induced defect clusters in fcc and bcc metals, mostly in copper and iron and have concluded that the radiation effects are considerably different between fcc and bcc metals [1]. However, a number of issues are remaining to be clarified. For example:

(1) Molecular dynamics (MD) simulation of cascades has given a displacement damage function almost common to any fcc, bcc and hcp metals and alloys, including intermetallics [2].

(2) Number density of defect clusters in copper under neutron irradiation grows much faster than in bcc iron. Many orders of magnitude larger fluence is required for iron to produce the same concentration of defect clusters in copper. In fact, almost no vacancy clusters are observed in irradiated iron. However, there are quantitative difference among bcc metals, e.g. in iron and molybdenum. As to the differences in vacancy cluster formation, another interpretation than the difference in crystal structure may be possible [3,4].

(3) Even among fcc metals, behaviour of copper and nickel is very much different. Accumulation of defect clusters in nickel is much slower than in copper. Vacancy clusters directly formed in a cascade are difficult to be observed in nickel [5]. Whether the behaviour in nickel is an exceptional case or not is not clear. The difference among fcc metals has been rationalised by assuming differences in cascade collapse efficiency and in intracascade clustering efficiencies of both types of point defects [1], but reasoning of these differences has not been given yet.

* Corresponding author. Tel.: +81-463 58 1211; fax: +81-463 50 2017.
E-mail address: ishino@keyaki.cc.u-tokai.ac.jp (S. Ishino)

0022-3115/00/$ - see front matter
PII: S0022-3115(99)00177-4

All these issues cast doubt about the existence of substantial differences among fcc and bcc metals. Ascribing the differences in radiation behaviour to the difference in crystal structure might be an oversimplifying assumption. It should also be pointed out that among the property changes taken for comparison [1], loop formation, void swelling and mechanical property changes are for high fluence irradiations, where complexities may come in to extract the crystal structure effects as unambiguously as possible.

In the present paper, we compare earlier results [6–9] of ion irradiation on fcc nickel and bcc iron in the light of differences in crystal structure. These metals are situated very closely in the periodic table, having not much different melting points and fairly strong electron–phonon coupling, both ferromagnetic and yet with different crystal structure. Therefore, more reliable comparison can be made than to compare fcc copper and bcc iron or molybdenum. In the present paper, we utilize the results of electrical resistivity measurements during and after irradiation at low temperature, where point defect clustering into a large dislocation loop does not take place extensively. Electrical resistivity measurements at low temperature can provide information on the total number of displacements no matter what their configurations are, so that we can look into the problem of defect production from the different angle. Justification of utilizing electrical resistivity measurements for deriving total number of displacements has been discussed in another paper [10]. We have had a unique opportunity to use various kinds of accelerators, which have enabled us to irradiate specimens at various temperatures from cryogenic to high temperatures with electrons, light and heavy ions of energies ranging from 1 MeV to more than 100 MeV. Such wide variety of ion irradiations, giving a wide variety of defect configurations from simple Frenkel pairs to clustered defects in a cascade, will give insight on production, annihilation, accumulation and evolution of irradiation induced defects under different irradiation conditions in terms of nuclear as well as electronic energy deposition. By using the electrical resistivity measurements, one of the authors (A.I.) and his coworkers have modified conventional method of analysis [11], and have established methods to derive damage production cross sections, defect annihilation cross sections during irradiation, damage efficiency together with specific kinetic parameters of defect annealing stages [12].

In Section 2, we will summarise the experimental procedures and the way how we derive damage parameter values useful for comparison between nickel and iron. These damage parameters as damage production cross sections and radiation induced defect annihilation cross sections for nickel and iron are re-analysed and compared. Both metals behave similarly as far as these parameters are concerned in most cases and the difference in crystal structure may not be an essential factor. In the case of irradiations with energetic heavy ions in 100 MeV range, annihilation cross section can be scaled in terms of electronic stopping power. Moreover, in the case of iron, the damage production cross section deviates from the trend for lower energy ion irradiations. Electronic energy deposition may play an important role even for low energy ions as well as for high energies. Discussion will be given on the effect of electronic energy deposition on defect clustering, i.e. so called cascade yield in Section 4.

2. Experimental procedures and the method of analyses

Low energy (~1 MeV) and high energy (~100 MeV) ions were irradiated in thin film nickel and in iron at low temperatures. In all cases studied, ranges of the incident ions exceed the film thickness, so that the remaining implanted impurities can be neglected. Electrical resistivity measurements were made in situ at low temperature by a conventional four point probe technique to derive damage production and annihilation cross sections. To convert the resistivity change to defect concentration, literature values of resistivity contribution for unit concentration of Frenkel pairs of 1250 μΩ cm [13] and 600 μΩ cm [14,15] were used for iron and nickel, respectively.

2.1. Ion irradiations in nickel

Polycrystalline nickel films of 200–500 nm thick were evaporated using 99.998% pure nickel obtained from Johnson-Massey Company on an anodised aluminium plate with oxide thickness of about 200 nm. The specimen shape with current and potential electrodes was defined by stainless steel masking.

The specimens were irradiated with low energy (~1 MeV) ions from a 2 MV van de Graaff accelerator, and with high energy (~100 MeV) ions from a 20 MV tandem accelerator, both at JAERI-Tokai. Low energy ions used were ^{1}H, ^{3}He,^{4}He, ^{14}N, ^{40}Ar in the energy range between 0.5 and 1.82 MeV, high energy ions being ^{12}C, ^{19}F, ^{28}Si, ^{35}Cl, ^{81}Br, ^{127}I with energies ranging from 84 to 126 MeV. Irradiation temperature was below 10 K.

The beam current was 20–50 particle nano-amperes (pnA) for low energy H and He ions, 1–5 pnA for low and high energy heavy ions. The total resistivity change was about 0.5 μΩ cm, i.e. ~0.8 mdpa.

2.2. Ion irradiations in iron

Polycrystalline iron thin films of about 190–370 nm thick were deposited on alpha-alumina single crystal substrates by rf magnetron sputtering with a 99.99%

pure Fe target using Ar gas. Electrical resistivity of the specimens at room temperature was typically 10 μΩ cm.

The specimens were irradiated with low energy ions; 0.5 MeV ^{1}H, 1.0 MeV^{4}He, 1.0 MeV^{12}C, 1.0 MeV ^{20}Ne and 2.0 MeV^{40}Ar from a 2 MV Van de Graaff accelerator, and with high energy ions; 120 MeV^{35}Cl, 150 MeV ^{58}Ni, 125 MeV ^{79}Br, 185 MeV ^{127}I, 200 MeV ^{127}I and 200 MeV ^{197}Au from a 20 MV tandem accelerator at JAERI-Tokai. Irradiations were performed at liquid nitrogen temperature (~80 K) to suppress thermal motion of irradiation produced defects.

The beam current was similar to the case of nickel irradiations given above, namely, 20–50 particle nanoamperes (pnA) for low energy H and He ions, 1–5 pnA for low and high energy heavy ions. The total resistivity change was about 0.3 μΩ cm (~0.24 mdpa) in most cases.

2.3. Electrical resistivity measurements and the method of analyses

In situ electrical resistivity measurements were performed during irradiation at appropriate fluence intervals. The specimen temperature was kept below 10 K for nickel, and ~80 K for iron. Since Stage I recovery temperature for pure iron is high, defect recovery between ~10 K and ~80 K is small. This will justify the comparison between 10 K-irradiated nickel and 80 K-irradiated iron. Post irradiation annealing was performed during warm up with a constant rate of increasing the temperature of 1.5–2 K/min.

The rate of change in resistivity, $[\mathrm{d}(\Delta\rho)/\mathrm{d}\Phi]$, can be expressed as

$$\ln\left(\frac{\mathrm{d}(\Delta\rho)}{\mathrm{d}\Phi}\right) = \ln(\rho_{\mathrm{F}}\sigma_{\mathrm{d}}) - \sigma_{\mathrm{r}}\Phi,$$

where $\Delta\rho$ is the increase in resistivity, Φ the ion fluence [8].

By plotting $\log[\mathrm{d}(\Delta\rho)/\mathrm{d}\Phi]$ vs. Φ, damage production, σ_{d} and defect annihilation cross sections, σ_{r} can be derived. For high energy ion irradiations, there are more than one type of defects with different stability against radiation annealing. The defect annihilation cross section for each defect can be separately obtained by analyzing the $\log[\mathrm{d}(\Delta\rho)/\mathrm{d}\Phi]$ vs. Φ curve.

3. Comparison of ion irradiation results for nickel and iron

3.1. Damage production cross section for low energy ions

Damage production cross section σ_{d} , which is a cross section for the production of total displacements, can be derived from the rate of change in resistivity at zero fluence divided by ρ_{F}, the resistivity contribution for unit concentration of Frenkel pairs. The damage production cross sections for low energy ion irradiations for Ni and Fe as a function of damage energy are shown in Fig. 1. The damage energy, which is the energy deposited into nuclear motion eventually at the end of the cascade initiated by the incident ion, is approximated here by the nuclear energy deposition for incident ion, i.e. the elastic energy loss per unit length.

It is clear that log–log plot of damage production cross section vs. damage energy gives a straight line with exponent of 0.86–0.90. There are no differences in the behaviour of nickel and iron. This is closely related to the results of MD simulation [2], where the exponent of the log–log plot of the number of Frenkel pairs against damage energy is in the range of 0.71–0.80. In this case, the damage energy is the PKA energy subtracted by the total electronic energy loss in the cascade. Another thing to note is that the energy range of the MD calculations is below ~50 keV, whereas in our case, energy range is much wider.

3.2. Damage production cross section for high energy ions

Fig. 2 shows damage production cross sections for both low energy (~MeV) and high energy (~ 100 MeV) ions in iron(◯,●) and nickel (□, ■) as a function of damage energy. Open symbols are for low energy ions, closed symbols being for high energy ions.

It is obvious from Fig. 2 that for irons solid circles for higher damage energies are plotted above the low energy line, whereas for nickel, solid squares for higher damage energies lie below the low energy line. These deviations appearing only for higher energies differ in iron and nickel. However, the difference may not be due to the difference in crystal structure. Most probable explanation will be the effect of electronic excitation as discussed in Section 4.

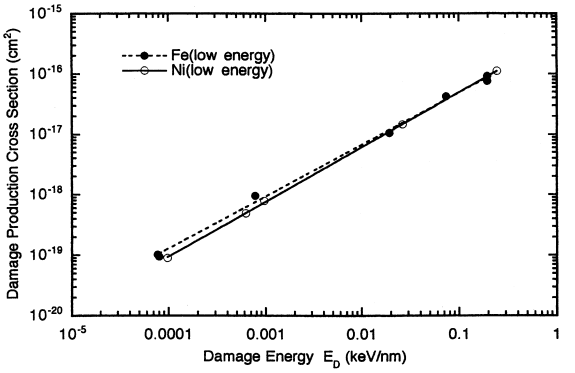

Fig. 1. Damage production cross section as a function of damage energy for irradiation with low energy (~MeV) ions in iron (●) and in nickel (◯).

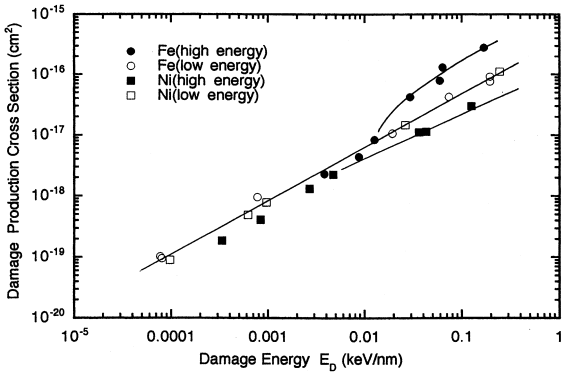

Fig. 2. Damage production cross section as a function of damage energy for irradiation with high (~100 MeV) (●) and low (~MeV) (○) energy ions in iron and high (■) and low (□) energy ions in nickel.

3.3. Fraction of Stage 1 recovery

Before irradiation, temperature dependence of resistivity was measured from low temperature with a constant warm-up rate of 1.5–2 K/min. After irradiation at low temperature, the resistivity of the specimens was measured during warming-up at the same warm-up rate. The difference in resistivity between the two runs gives annealing stages [6,9,12]. Fig. 3 shows the fraction of Stage I recovery as a function of damage energy for low energy ion irradiations.

There is a slight recovery as a part of Stage I recovery below the irradiation temperature of 80 K in iron, but the fraction may be less than 20%. In the case of nickel, irradiations were performed around 10 K, which is below the Stage I recovery temperature for nickel. The amount of defects introduced by irradiation before annealing was 240 ppm for iron, 800 ppm for nickel.

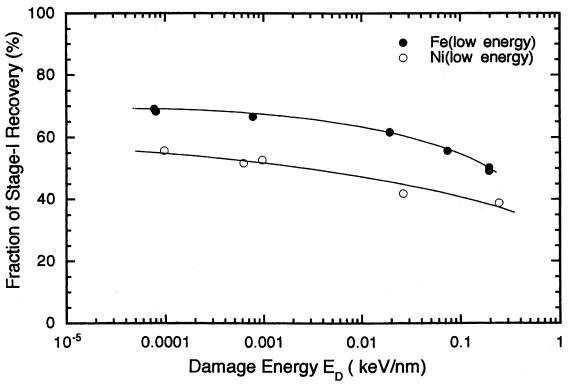

Fig. 3. Fraction of Stage I recovery as a function of damage energy for irradiation with low energy (~MeV) ions in iron (●) and in nickel (◯).

Although differences in the amount of irradiation induced defects, in specimen preparation, in irradiation temperature and so on will prevent us from direct comparison between two metals. A general trend that the Stage I fraction decreases gradually as the damage energy increases is observed for both metals. The results indicate that the fraction of close Frenkel pairs decreases increasing damage energy for low energy ion irradiations. Annealing studies after irradiation with high energy heavy ions in various fcc metals have been reported [12]. Those for bcc metals are under way. As mentioned in the previous section, damage production in iron becomes higher for high energy ion irradiations. Dunlop et al. have also found increased damage production for irradiation with ions of GeV energy range [16].

3.4. Defect annihilation cross section

The cross section for radiation induced defect annihilation, σ_r as defined in Section 2.3, is obtained by analyzing non-linear defect accumulation curves as explained briefly in Section 2. For low energy ion irradiations, defect annihilation cross sections as a function of damage energy are almost identical for iron and nickel as shown in Fig. 4. For high energy ion irradiations, annihilation processes are not simple. There are multiple cross sections for different defects responsible for the annihilation [7,8]. As far as nuclear stopping plays a major role in radiation effects, radiation induced annihilation behaviour does not seem to depend on crystal structure. Complex annihilation behaviour for high energy ion irradiations can be correlated well with the electronic stopping power both in fcc metals [7] and in bcc iron [8].

3.5. Damage efficiency

Damage efficiency, ξ as defined by

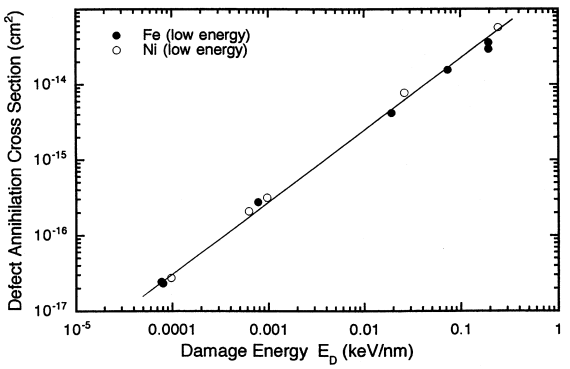

Fig. 4. Defect annihilation cross section as a function of damage energy for low energy ion irradiations in iron (●) and in nickel (◯).

$$\xi = \sigma_d^{exp}/\sigma_d^{calc}$$

is shown in Fig. 5 as a function of PKA median energy, $T_{1/2}$. for low energy ion irradiations in iron and nickel. Here, σ_d^{calc} is calculated by using the TRIM-92 computer code [17] with threshold energies of 24 eV for iron [13], 33 eV for nickel [18]. The PKA median energy is defined as the PKA energy up to which 50% of the total dpa is created [19].

The damage efficiency decreases with increasing PKA energy and levels off above around 10 keV at a value of $\xi \sim 0.3$, which is qualitatively consistent with a number of previous publications [20–22]. However, the absolute value of the efficiency has some ambiguity. Since for low energy light ion irradiations, the efficiency should be close to one, the efficiency values are normalised for low energy proton irradiations. Fig. 6 shows the normalised damage efficiency including the efficiency values for high energy ion irradiations. From the figure, the findings are summarised as follows:

1. There are no fundamental differences in normalised damage efficiency for low energy ion irradiations in iron and nickel (Compare ◯ and □).
2. In iron, high energy ion irradiations give abruptly increasing damage efficiencies as compared with those for low energy ion irradiations even though PKA median energy is in the same order of magnitude (Compare ◯ and ●).
3. In nickel, high energy ion irradiations give lower damage efficiencies than those for low energy ion irradiations (Compare □ and ■).

It is interesting to note that the damage efficiency in iron for high energy ion irradiations exceeds the value of one, i.e. the damage production by nuclear energy deposition. The defects giving the surplus resistivity are being investigated by annealing experiments.

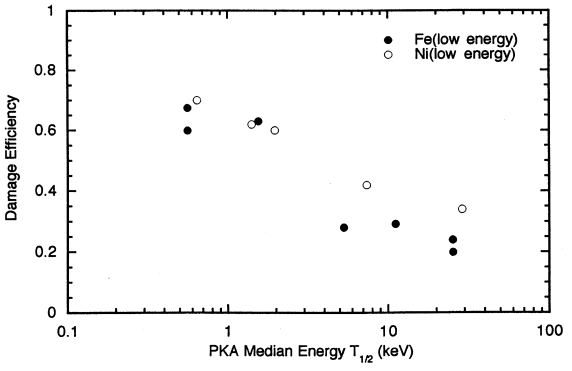

Fig. 5. Damage efficiency as a function of PKA median energy for low energy ion irradiations in iron (●) and in nickel (◯).

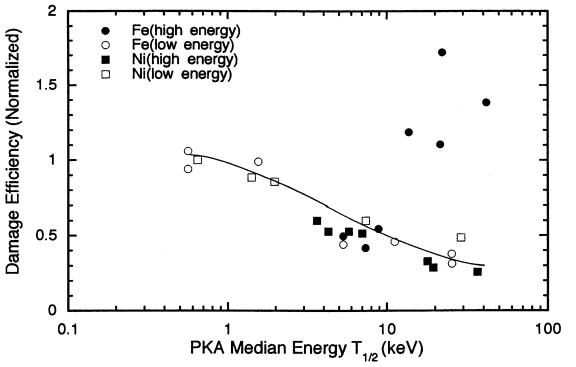

Fig. 6. Damage efficiency as a function of PKA median energy for irradiation with high (~100 MeV) (●) and low (~MeV) (○) energy ions in iron and high (■) and low (□) energy ions in nickel, normalized for low energy protons to be 1.

4. Discussion

4.1. Effects of crystal structure

Problems of radiation effects on materials cover extremely wide range; timewise from $\sim 10^{-15}$ to 10^{9} s and spacewise from $\sim 10^{-14}$ to 10^{2} m (in some case 10^{7} m) [23,24]. Time and space are intercorrelated as shown in Fig. 7. Generally speaking, the effect of crystal structure will appear for the correlated length greater than interatomic spacing and the corresponding time longer than $\sim 10^{-16}$ s.

Radiation damage process comprises a series of events:

1. nuclear encounter, producing a PKA,
2. collisional phase of a cascade,
3. cooling phase of the cascade,
4. thermal stage of the cascade, i.e. thermalization process within the cascade,
5. diffusional phase, i.e. thermally activated defect processes outside the cascade,

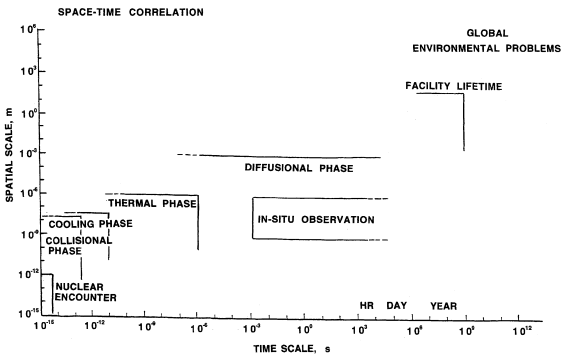

Fig. 7. Space and time correlation for radiation effects.

6. further defect evolution with associated property changes.

The events (1) and (2) should be immune to crystal structure effect, whereas events (5) and (6) should depend on crystal structure. The present paper is mostly concerned with damage production cross section, defect annihilation cross section and damage efficiency. These are related to the series of events up to (4) given above. It is interesting to note that these do not depend strongly on crystal structure at least for low energy ion irradiations. Differences between nickel and iron did arise in the fraction of Stage I recovery for low energy ion irradiations and damage production cross section and damage efficiency for high energy ion irradiations. The former differences may arise, at least partly, from the difference in crystal structure because of the differences in defect configurations and in recombination volume, i.e. in the stability of Frenkel pairs. However, general trend of the dependence of the fraction of Stage I recovery on damage energy is similar, implying that physics behind is essentially similar.

4.2. Effect of electronic excitation

The latter differences observed in high energy ion irradiations may be due to electronic stopping. Iwase and Iwata have observed increased damage efficiency for high energy ion irradiations in copper and silver which have weak electron–phonon coupling and reduction of damage efficiency in nickel and platinum, which are thought to have strong electron–phonon coupling [7], though there is an indirect evidence from ion beam mixing experiment that the electron–phonon coupling in Ni, Pd and Pt is not as large as has previously been considered [25]. Iwase and Iwata have accounted the enhanced production in Cu and Ag to the mutual Coulomb repulsion of ions positively charged by electronic excitation and the reduction of damage efficiency in nickel and platinum to enhanced transfer of energy from electronic to lattice system by strong electron–lattice coupling, which will give enhanced annihilation of Frenkel pairs. In the present report, however, enhanced damage efficiency occurs in iron which has strong electron–lattice coupling. (Here, we use intentionally the term 'electron–lattice coupling' because the relevant effect might occur within much shorter time than that required for the phonon normal mode to be set up, which is of the order of several times of the reciprocal Debye frequency, ν_D^{-1}. Small scale MD calculations of cascades for low energy PKAs (250 eV) have indicated that highly disturbed state may continue at least for a fraction of a picosecond [23,26].) Therefore, in the case of iron irradiated with high energy ions, another mechanism than in the case of copper must be sought for. One of the possibilities, as proposed by Dunlop et al. [16], is the presence of allotropic transformation in iron. Because of the strong electron–lattice coupling, lattice temperature will increase rapidly, exceeding phase transition temperature and then quenched. During the course of this temperature excursion, defects might be formed because phonon soft mode at the transition will facilitate the defect formation [27].

In order for the above explanations to be operative, time structure of dissipation of energy mainly given to the electronic system originally must be taken into account in the case of high energy ion irradiations. Fig. 8 shows the time scale of some relevant interactions involved in swift heavy ion irradiations in order to consider energy deposition, relaxation within the electronic system, transfer of energy from electronic to lattice system and evolution within the lattice system. Time required for self ions of various energies to traverse atomic-size length (typically represented by Bohr screening radius, a_B), i.e. a_B/v is also shown for several energies of self ions in copper as a basic frame of time, where v is the relative velocity between the incident particle and the target atom.

Electronic excitation by contact interaction (as δ-ray production) should occur in a time scale of a_B/v, the typical value of which is $\sim 10^{-17}$ s for 100 MeV self ions. This value is taken as the time required for the incoming ion to give its energy to the electron gas [28]. Energy deposited in electronic system will be shared with other electrons in 10^{-15}–10^{-14} s [29]. This time scale is also characteristic for de-excitation of inner shell vacancy with intermediate to outer shell electrons. Reciprocal of plasmon frequency, ω_p^{-1}, may give a characteristic response time, τ_p for the electron gas; $\tau_p = 2\pi\omega_p^{-1} \sim 10^{-16}$s [30,31]. Interaction between electron and atom has a characteristic time of the order of 10^{-13}–10^{-12} s [32]. This is also typical for electron–phonon relaxation time, whereas phonon–phonon relaxation time is much longer ($\sim 10^{-11}$ s) [33]. Extremely short time measurement has become possible with femtosecond lasers [34] and

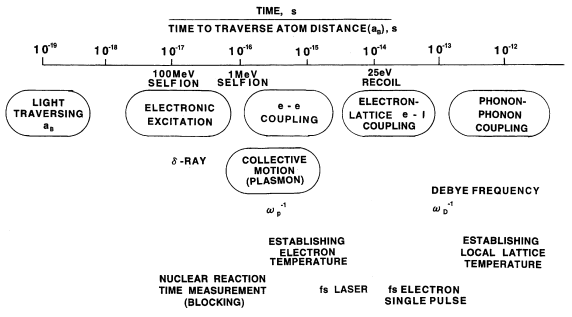

Fig. 8. Time scale of some relevant interactions for energy relaxation in electronic and lattice systems. Time required for self ions of various energies to traverse one atomic distance (represented by Bohr radius, a_B) is also shown.

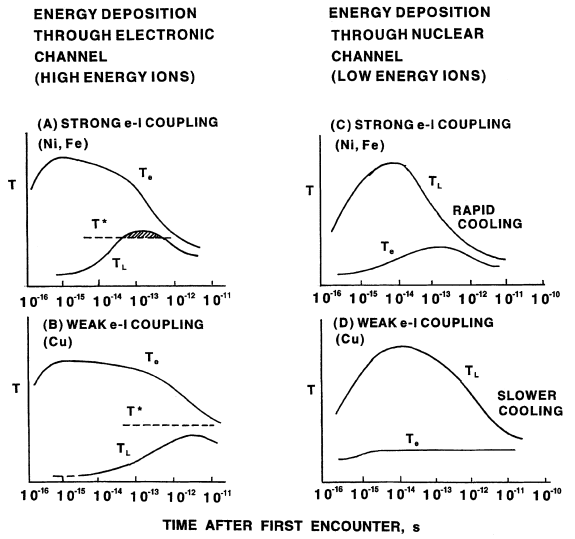

Fig. 9. Time evolution of electron (T_e) and lattice temperatures (T_L) for high energy (A,B) and low energy (C,D) ion irradiations in materials with strong (A,C) and weak (B,D) electron–lattice coupling.

blocking techniques [35,36]. These are also shown in the figure.

Now, let us consider energy deposition, relaxation and transfer in electronic and lattice systems during and after impingement of energetic heavy particles.

Because the characteristic time constants for energy deposition and relaxation are so short, it would be difficult to define the temperature of the electronic and lattice systems [37]. Here, we use notations, T_e and T_L, and the terminology of 'temperature' simply to represent local energy densities in electronic and lattice systems divided by the Boltzmann constant.

Under this assumption, one can draw time evolution of electron (T_e) and lattice temperatures (T_L) as shown in Fig. 9 for high energy and low energy ion irradiations in materials with strong and weak electron–lattice coupling. Similar analysis has been made by Wang et al. [37]. There are characteristic local energy densities, hence characteristic 'temperature' denoted by T^* at which phase transformations as melting or allotropic transformations occur. Dunlop et al. have presented the idea that displacive transformation favours an efficient transfer of energy between highly excited electrons and target atoms [38].

In the following, we will briefly discuss time evolution of electron (T_e) and lattice temperatures (T_L) in four cases, namely for high and low incident ion energies onto target materials with strong and weak electron–lattice coupling:

- In case A (high energy–strong electron–lattice coupling case), energy deposited into electronic systems can be effectively used to heat the lattice. Therefore, even if defects are formed by Coulomb repulsion, annihilation occurs quickly. However, if there are some critical points and the lattice temperature will exceed the critical point, defects might be created. This explains reduced damage efficiency in nickel. Iron, which has allotropic transformation, might be an example of the special case; once the lattice temperature exceeds the critical point, creation of defects might occur, leading to the enhanced damage efficiency in the case of iron.
- In case B (high energy–weak electron–lattice coupling case), high density electronic excitation will produced defects by Coulomb repulsion (Coulomb explosion model). Because of slow rise of lattice temperature, thus produced defect will survive. In fact, defect production by strong electronic excitation has been observed [7]. However, the phenomenon appears more prominently in thinner foils [7]. Exact nature of this specimen thickness dependence, together with the conditions for the appearance of Coulomb explosion are interesting subjects to be clarified.

Case C and D are for low energy ion irradiations, where energy is mostly deposited into lattice system so that at least in early stage T_L is higher than T_e.

- In case C (low energy–strong electron–lattice coupling case), because of the strong electron–lattice coupling, lattice temperature cools down rapidly. There are not many differences in nickel and iron.
- In case D (low energy–weak electron–lattice coupling case), energy in the lattice system is dissipated slowly so that the cascade cooling is slow. This will facilitate formation of collapsed vacancy loops or tetrahedra. Only such extended defects can be observed by transmission electon microscopy.

In low energy ion irradiations, defect yield, which is the number of vacancy clusters per incident ion has been studied [1,39]. A number of researchers have discussed the importance of electron–phonon coupling to account for the observations [40,41]. The defect yields in copper, silver and gold are high, whereas that in nickel is low and iron is extremely low. These observations are consistent with the cases of C and D. Thus, the electronic energy deposition plays an important role even for low energy ions as well as for high energies.

5. Conclusions

1. Defect accumulation behaviour in Ni and Fe irradiated with low energy (~1 MeV) and high energy (~100 MeV) ions was studied by in situ electrical resistivity measurements below Stage I recovery temperatures, at 10 K for Ni, 80 K for Fe.
2. Damage production cross sections and the damage efficiency for low energy ions of MeV energy range

as a function of damage energy, or of PKA median energy are surprisingly similar in both metals; nickel and iron. This seems to agree with MD simulation results of displacement damage function.

3. For higher ion energies, typically 100 MeV or above, radiation induced annealing is observed even from early stage of irradiation in nickel, whereas in iron, enhancement of damage production is sometimes observed, probably depending on the degree of electronic stopping.
4. Difference in crystal structure does not seem to play a major role in the primary phenomena of damage production and radiation induced annealing observed. Instead, electron–phonon coupling, i.e. the way how the energy deposited in the electronic system relaxes may be important even for low energy ion irradiations.

Acknowledgements

In the present paper, we have analysed the experimental results published earlier. The authors are grateful for the colleagues of one of the authors (A.I.), particularly Drs T. Iwata, Y. Chimi and N. Ishikawa for the use of the experimental results.

References

[1] B.N. Singh, J.H. Evans, J. Nucl. Mater. 226 (1995) 277.
[2] D. Bacon, A.F. Calder, F. Gao, J. Nucl. Mater. 251 (1997) 1.
[3] K. Morishita, H.L. Heinisch, S. Ishino, N. Sekimura, J. Nucl. Mater. 212–215 (1994) 198.
[4] K. Morishita, H.L. Heinisch, S. Ishino, N. Sekimura, Nucl. Instrum. and Meth. B 102 (1995) 67.
[5] S. Ishino, K. Fukuya, T. Muroga, N. Sekimura, H. Kawanishi, J. Nucl. Mater. 122&123 (1984) 597.
[6] A. Iwase, A. Sasaki, T. Iwata, T. Nihira, Phys. Rev. Lett. 58 (1987) 2450.
[7] A. Iwase, T. Iwata, Nucl. Instrum. and Meth. B 90 (1994) 322. See also references therein.
[8] Y. Chimi, A. Iwase, N. Ishikawa, Mater. Res. Soc. Symp. Proc. 504 (1999) 221.
[9] Y. Chimi, A. Iwase, N. Ishikawa, J. Nucl. Mater. 271&272 (1998) 236.
[10] T. Iwata, A. Iwase, Radiat. Eff. Def. Solids 144 (1998) 27.
[11] See for example, H. J. Wollenberger, Vacancies and Interstitials in Metals, in: A. Seeger, D. Schumacher, W. Schilling, J. Diehl (Eds.), North-Holland, Amsterdam, 1970, p. 215.
[12] See for example, T. Iwata, A. Iwase, Radiat. Eff. Def. Solids, 113 (1990) 135.
[13] P.G. Lucasson, R.M. Walker, Phys. Rev. 127 (1962) 485.
[14] P. Ehrhart, W. Schilling, Phys. Rev. B 8 (1978) 2604.
[15] F.W. Young Jr., J. Nucl. Mater. 69&70 (1978) 310.
[16] A. Dunlop, D. Lesueur, P. Legrand, H. Dammak, J. Dural, Nucl. Instrum. and Meth. B 90 (1994) 330.
[17] Original version of TRIM is reported in J.P. Biersack, L.G. Haggmark, Nucl. Instrum. and Meth. 174 (1980) 257.
[18] P. Lucasson, in: Proceedings of the International Conference on Fundamental Aspects of Radiation Damage in Metals, USERDA, CONF-751006-p1, vol. 1 1976 p. 42.
[19] R.S. Averback, R. Benedek, K.L. Merkle, Phys. Rev. B 18 (1978) 4156.
[20] R.S. Averback, J. Nucl. Mater. 108&109 (1982) 33.
[21] T. Muroga, S. Ishino, J. Nucl. Mater. 117 (1983) 36.
[22] T. Muroga, S. Ishino, P.R. Okamoto, H. Wiedersich, J. Nucl. Mater. 122&123 (1984) 634.
[23] S. Ishino, J. Nucl. Mater. 206 (1993) 139.
[24] N. Sekimura, Nuclear Energy and Advanced Technology-1, NSA/Commentaries, No.2 (1994) (in Japanese). See also K. Morishita, N. Sekimura and T. Diaz de la Rubia, J. Nucl. Mater. 248 (1997) 400.
[25] K. Nordlund, L. Wei, Y. Zhong, R.S. Averback, Phys. Rev. B 57 (1998) R13965.
[26] K. Morishita, N. Sekimura, T. Toyonaga, S. Ishino, J. Nucl. Mater. 191–194 (1992) 1123.
[27] A. Dunlop, P. Legrand, D. Lesueur, N. Lorenzelli, J. Morillo, A. Barbu, S. Bouffard, Europhys. Lett. 15 (1991) 765.
[28] Ch. Dufour, Z.G. Wang, M. Levalois, P. Marie, E. Paumier, F. Pawlak, M. Toulemonde, Nucl. Instrum. Meth. B 107 (1996) 218.
[29] E. Paumier, M. Toulemends, J. Dural, J.P. Girard, P. Bogdanski, C. Dufour, R. Carin, A. Hairie, D. Julienne, M. Levalois, R. Madelon, M.N. Metzner, Mater. Sci. Forum 97–99 (1992) 599.
[30] A. Dunlop, D. Lesueur, Mater. Sci. Forum 97–99 (1992) 553.
[31] D. Lesueur, A. Dunlop, Radiat. Eff. Def. Solids 126 (1993) 163.
[32] S.D. Brorson, A. Kazeroonian, J.S. Moodera, D.W. Face, T.K. Cheng, E.P. Ippen, M.S. Dresselhous, G. Dresselhaus, Phys. Rev. Lett. 64 (1990) 2172.
[33] C. Kittel, Introduction to Solid State Physics, 1st ed., Wiley, New York, 1953, p. 243.
[34] M. Uesaka, T. Watanabe, T. Ueda, M. Kando, K. Nakajima, H. Kotaki, A. Ogata, J. Nucl. Mater. 248 (1997) 380.
[35] M. Maruyama, K. Tsukada, K. Ogawa, F. Fujimoto, K. Komaki, M. Mannami, T. Sakurai, Nucl. Phys. A 145 (1970) 581.
[36] F. Fujimoto, K. Komaki, M. Maruyama, K. Ogawa, Y. Sugiyama, Nucl. Instrum. Meth. 132 (1976) 175.
[37] Z.G. Wang, Ch. Dufour, E. Paumier, M. Toulemonde, Phys.: Condens. Matter 6 (1994) 6733.
[38] A. Dunlop, P. Legrand, D. Lesueur, N. Lorenzelli, J. Morillo, A. Barbu, S. Bouffard, Europhys. Lett. 15 (7) (1991) 765.
[39] K. Morishita, H.L. Heinisch, S. Ishino, N. Sekimura, J. Nucl. Mater. 212–215 (1994) 198.
[40] I.M. Robertson, D.K. Tappin, M.A. Kirk, Philos. Mag. A 68 (1993) 843.
[41] D.K. Tappin, I.M. Robertson, M.A. Kirk, Mater. Res. Soc. Symp. Proc. 373 (1995) 41.